Basic Res Cardiol (2011) 106:371–383
DOI 10.1007/s00395-011-0157-0

ORIGINAL CONTRIBUTION

Cardiac-specific overexpression of E3 ligase Nrdp1 increases ischemia and reperfusion-induced cardiac injury

Yuan Zhang · Yong Zeng · Min Wang · Cui Tian · Xu Ma · Houzao Chen · Quan Fang · Lixin Jia · Jie Du · Huihua Li

Received: 6 August 2010 / Revised: 28 December 2010 / Accepted: 25 January 2011 / Published online: 11 February 2011

Abstract Cardiomyocyte death is a major event of myocardial infarction. Previously, we and others have shown that E3 ligase-mediated protein turnover plays a critical role in cardiac injury. In this study, we sought to determine the role of a newly identified E3 ligase, neuregulin receptor degradation protein-1 (Nrdp1), on cardiac ischemia/reperfusion (I/R) injury. I/R injury markedly upregulated Nrdp1 expression in heart tissue. To elucidate the role of Nrdp1 in I/R-induced cardiac injury, neonatal cardiomyocytes were infected with adenoviral constructs expressing wild-type, dominant-negative Nrdp1 genes. Increased Nrdp1 expression enhanced I/R-induced cardiomyocyte apoptosis and inflammation as compared with the green fluorescent protein (GFP) control; these effects were attenuated by overexpression of a dominant-negative Nrdp1 (C34S/H36Q). Furthermore, cardiac-specific Nrdp1 overexpression in vivo in mouse significantly increased infarct size, the number of TUNEL-positive nuclei and inflammatory cells, as well as mortality, as compared with wild-type mice after I/R injury. The mechanisms underlying these effects were associated with the downregulation of an Nrdp1 substrate, ErbB3, accompanied by suppression of its downstream targets AKT, ERK1/2, and activation of p38 and JNK1/2. Together, these results provide evidence for an important role for Nrdp1 in regulating I/R-induced cardiac injury. Nrdp1 may constitute a new therapeutic target for ameliorating the I/R-induced cardiac injury.

Keywords Nrdp1 · Myocardium · Ischemia/reperfusion · Apoptosis · Inflammation

Y. Zhang and Y. Zeng contributed equally to this work.

Electronic supplementary material The online version of this article (doi:10.1007/s00395-011-0157-0) contains supplementary material, which is available to authorized users.

Y. Zhang · M. Wang · H. Chen
Department of Pathology, National Laboratory of Medical Molecular Biology, Institute of Basic Medical Sciences, Chinese Academy of Medical Sciences and Peking Union Medical College, Beijing 100005, China

Y. Zeng · Q. Fang
Department of Cardiology, Peking Union Medical Hospital, Beijing 100730, China

C. Tian · H. Li (✉)
The Key Laboratory of Remodeling-Related Cardiovascular Diseases, Department of Pathology, School of Basic Medical Sciences, Capital Medical University, No. 10 Xitoutiao, You An Men, Beijing 100069, China
e-mail: hhli1935@yahoo.cn

X. Ma
Department of Genetics, National Research Institute for Family Planning, Beijing 100081, China

L. Jia · J. Du (✉)
The Key Laboratory of Remodeling-Related Cardiovascular Diseases, Capital Medical University, Ministry of Education, Beijing Institute of Heart Lung and Blood Vessel Diseases, Beijing Anzhen Hospital Affiliated the Capital Medical University, Beijing 100029, China
e-mail: jdu@bcm.edu

Introduction

Ischemic heart disease, including myocardial infarction, is the major cause of death in the world. One of the most important prognostic factors is the development of left ventricular (LV) remodeling, which includes cardiac hypertrophy, cardiac fibrosis, and subsequent LV dysfunction leading to heart failure [24]. Emerging evidence demonstrates that LV remodeling after myocardial infarction is associated with cell apoptosis and intense inflammatory response to cytokine release and cardiac infiltration of immune cells [15, 20]. Apoptosis and inflammation are regulated by specific proteolytic systems, and the ubiquitin–proteasome system plays a critical role in mediating cellular protein degradation in cardiac disease [18, 25]. Several E3 ubiquitin ligases, including carboxyl terminus of Hsc70-interacting protein (CHIP), murine double minute 2 (MDM2), muscle-specific RING finger protein 1 (MuRF1), and atrogin-1/muscle atrophy F-box (MAFbx), have been linked to parallel pro-apoptotic and survival pathways in cardiomyocytes [16, 18, 30, 36].

Neuregulin receptor degradation protein-1 (Nrdp1, also known as FLRF or RBCC), is a RING finger E3 ubiquitin ligase and primarily expressed in the heart, skeletal muscle and brain [7]. Nrdp1 promotes ubiquitination of several proteins such as ErbB3, BRUCE/apollon, MyD88, TBK1, and Parkin, thereby regulating cell growth, apoptosis, and inflammation [5, 7, 26, 27, 31]. Given that apoptosis and inflammation are the major events in the process of cardiac injury, we investigated the role of Nrdp1 in ischemia/reperfusion (I/R)-induced cardiomyocyte injury in vitro and whether Nrdp1 overexpression could enhance cardiac I/R injury in vivo.

Materials and methods

Antibodies and reagents

Antibodies used: Nrdp1 (BETHYL Laboratories, Inc.), Flag and α-actinin (Sigma-Aldrich), Bax, Bcl-2, cleaved caspase-3, cleaved PARP, phospho-ErbB3 (Tyr1289), total and phospho-AKT (Ser473), total and phospho-ERK1/2 (Thr202/Tyr204), total and phospho-STAT3 (Tyr705), total and phospho-p38 (Thr180/Tyr182), total and phospho-JNK1/2 (Thr183/Tyr185), MyD88, TBK1 and horseradish peroxidase-conjugated goat anti-mouse or anti-rabbit IgG antibody (Cell Signaling Technology), BRUCE (BD Biosciences), ErbB3 (sc-285) and β-actin (Santa Cruz Biotechnology). Other reagents were purchased from Sigma-Aldrich.

Adenoviral constructs, cell culture and simulated I/R protocol

The cDNA encoding full-length mouse Nrdp1 with a Flag epitope tag or dominant-negative Nrdp1 (C34S/H36Q) mutant [7, 26] (gift of Dr. Xiaobo Qiu, College of Life Sciences, Beijing Normal University) was amplified by PCR. Recombinant adenoviruses expressing green fluorescent protein (GFP) alone (Ad-GFP), Nrdp1 (Ad-Nrdp1) and dominant-negative (Dn) Nrdp1 (Ad-Dn-Nrdp1) driven by the cytomegalovirus promoter were generated by use of the AdEasy system (MP Biomedicals) [17]. Neonatal rat cardiomyocytes were isolated by enzymatic disassociation from 1-day-old Sprague–Dawley rats [17]. Twenty-four hours after plating, cells were infected with Ad-GFP, Ad-Nrdp1, or Ad-Dn-Nrdp1. After 24 h of adenovirus infection, the cells underwent simulated ischemia for 2 h by replacing the cell medium with an ischemia buffer, and reperfusion was accomplished by replacing the ischemic buffer with normal cell medium under normoxia conditions for 30 min or 24 h as reported previously [33].

Generation of transgenic mice

A full-length mouse Nrdp1 cDNA [7] with a Flag epitope tag (Nrdp1-Flag) was cloned 3′ to a 5.5 kb segment of the α-myosin heavy chain promoter (α-MHC) and 5′ to a 0.6 kb polyadenylation signal from the human growth hormone gene (Fig. 3a) carried in the pBluescript II SK vector (Stratagene) [17]. A 7.1-kb NotI DNA fragment was isolated, purified, and injected into the pronuclei of fertilized C57BL/6 J mouse eggs. Two independent founder lines (lower and higher copies) were identified by PCR with use of an upper primer from the Nrdp1 cDNA (5′-TG GCTGTCCTGCTTCTAT-3′) and a lower primer from Flag (5′-CACCGTCATGG TCTTTGT-3′) to amplify a 278-bp fragment spanning the junction between the Nrdp1 cDNA and Flag epitope tag. Western blot analysis involved anti-Flag or -Nrdp1 antibody to confirm expression of the Nrdp1 transgenes. Six to eight mice per genotype at each time point were used. All procedures were approved by and performed in accordance with the Animal Care and Use Committee of Peking Union Medical College. The investigation conformed to the Guide for the Care and Use of Laboratory Animals published by the US National Institutes of Health (NIH Publication No. 85-23, revised 1996).

Echocardiographic measurements

With mice under tribromoethanol sedation (0.25 mg/g intraperitoneally), we obtained images using a high-resolution Micro-Ultrasound system (Vevo 770, VisualSonics,

Toronto, Canada) equipped with a 30-MHz transducer as described [17]. All variables were measured in the parasternal long-axis view for at least five consecutive cardiac cycles and averaged from at least two measurements. The percentage of fractional shortening (FS) was calculated as follows: FS = [(LVEDD − LVESD)/LVEDD] × 100%.

Creation of myocardial I/R model

Ten- to 12-week-old Nrdp1-transgenic (TG6) mice and nontransgenic wild-type (WT) littermates underwent myocardial I/R [36]. Briefly, mice were anesthetized by intraperitoneal injection of pentobarbital sodium (60 mg/kg body weight) and then placed in a supine position and mechanically ventilated. The proximal portion of the left anterior descending coronary artery was occluded with an 8-0 silk suture. Regional ischemia was confirmed by visual inspection of a pale color in the occluded distal myocardium and electrocardiographic ST-segment elevation. After occlusion for 30 min, the suture was loosened and the myocardium was reperfused for 24 h. Other WT and TG6 mice underwent sham operation without coronary artery ligation.

Assessment of area at risk and infarct size

To evaluate the effect of Nrdp1 overexpression on the area at risk (AAR) and infarct size, separate groups of WT and TG2 animals were created. After 24 h of coronary artery ligation, 1% Evans Blue dye was perfused into the aorta and coronary arteries, with distribution throughout the ventricular wall proximal to the site of coronary artery ligation. Hearts were frozen for 15 min and cut into four transverse sections below the ligature. These sections were weighed and then incubated with a 1% 2, 3, 5-triphenyltetrazolium chloride (TTC) solution at 37°C for 20 min. The infarct area, the AAR, and the left ventricular (LV) area from each section were analyzed by use of NIH Image software (US National Institutes of Health, Bethesda, MD), multiplied by the weight of the section, and then totaled from all sections. The ratio of AAR to LV, infarct size to AAR, and infarct size to LV area was calculated [36].

Histological analysis and TUNEL assay

Hearts from WT and TG6 mice fixed in 10% formalin were routinely processed and paraffin embedded. Heart sections (5 μm) were stained with hematoxylin and eosin (H&E) [17]. Apoptosis of heart sections and cardiomyocytes was analyzed by the In situ Cell Death Detection Kit (TUNEL fluorescence FITC kit, Roche, Indianapolis, IN, USA) according to the manufacturer's instructions. The myocardium was stained with α-actinin. Primary antibody levels were visualized after incubation with secondary antibodies conjugated to Alexa Fluor 568 (Molecular Probes). Finally, the sections were stained with DAPI (Sigma-Aldrich). Fluorescence staining was viewed by confocal microscopy (magnification, ×200) (Leica, Germany). Six visual fields were randomly selected from each section, and the TUNEL-positive ratio was calculated as follows: TUNEL-positive ratio = (number of green nuclei/number of blue nuclei) × 100%.

RNA analysis

Total RNA was purified from cardiomyocytes and fresh hearts of WT mice with Trizol (Invitrogen). RNA samples (2 μg) were reverse-transcribed to generate the first-strand cDNA [17]. The transcript levels of TNF-α, IL-6, ErbB3 and GAPDH (as a control) were detected by semi-quantitative RT-PCR analysis. Primer sequences were as follows: TNF-α forward, 5′-AGATGTGGAACTGGCAGAGG-3′, reverse, 5′-GGGCTTGTCACTCGAGTTTT-3′; IL-6 forward, 5′-GCCACTGCCTTCCCTACTTC-3′, reverse, 5′-TTGGTCCTTAGCCACTCCTT-3′; ErbB3 forward, 5′-TTGACTGGAGGGACATCG-3′, reverse, 5′-TGGCAGCACTGGTTAGGA-3′); GAPDH forward, 5′-GTGCCGCCTGGAGAAACCT-3′; reverse, 5′-TTGCTGTAGCCGTATTCATTGTCATA-3′.

Immunohistochemistry

Immunohistochemical staining was performed as described [35]. The histological sections were localized in the ischemic border area. Heart sections were stained with an antibody against Nrdp1 (1:500 dilution), IgG control or ErbB3 (1:100). To assess infiltration of inflammatory cells, sections were stained with a macrophage-specific anti-mouse Mac-2 antibody (1:400 dilution, Santa Cruz Biotechnology) at 4°C overnight, then with horseradish peroxidase-conjugated goat anti-rabbit antibody. Peroxidase activity was visualized with use of diaminobenzidine, and the sections were counterstained with hematoxylin. The number of Mac-2-positive cardiomyocytes was counted and expressed as a percentage of total number of cardiomyocytes in six sequentially cut 5-μm sections of the ischemic lesion (magnification × 200) for each animal.

Western blot analysis

Heart tissues ($n = 5$) were removed from the ischemic border area 24 h after reperfusion, immediately frozen in the liquid nitrogen, and then homogenized in lysis buffer. Western blot analysis was performed as described [17].

Statistical analysis

Data are presented as mean ± SD. Comparison between groups involved Student's *t* test or one-way ANOVA. Analysis of survival after I/R injury involved the Kaplan–Meier method and comparison by a log-lank test. A $P < 0.05$ was considered statistically significant.

Results

Myocardial I/R injury increases Nrdp1 expression

To provide initial evidence that Nrdp1 is involved in myocardial I/R injury, mice were subjected to 30-min ischemia and 24-h reperfusion to induce myocardial infarction. As shown in Fig. 1a, myocardial I/R significantly increased Nrdp1 expression by 2.3-fold as compared with controls ($P < 0.05$). Immunohistochemical staining also demonstrated Nrdp1 protein level significantly increased in the ischemic areas of injured hearts as compared with control hearts (Fig. 1b). These data suggest that increased Nrdp1 expression may play a role in myocardial injury.

Effect of Nrdp1 on I/R-induced cardiomyocyte apoptosis and inflammation

To investigate whether increased or decreased Nrdp1 activity could affect I/R-induced cardiomyocyte apoptosis and inflammation, neonatal rat cardiomyocytes were infected with Ad-GFP, Ad-Nrdp1 or Ad-Dn-Nrdp1. The infection efficiency reached more than 90% after 24 h. Infected cells were subjected to ischemia for 2 h, then reperfusion for 24 h, and expression of exogenous Nrdp1 proteins was demonstrated by western blot analysis with anti-Flag antibody (Fig. 2b). TUNEL assay and western blot and RT-PCR analysis were used to examine the effect of Nrdp1 adenoviral transfection on cardiomyocyte apoptosis and inflammation in cells. The groups did not differ in apoptosis, Bax/Bcl-2 ratio or expression of TNF-α and IL-6 under the basal condition (Fig. 2a–c). However, after I/R treatment, overexpression of Nrdp1 enhanced cardiomyocyte apoptosis, Bax/Bcl-2 ratio, and the expression of TNF-α and IL-6 as compared with the GFP control; infection with the Dn-Nrdp1 mutant (lacking E3 ubiquitin ligase activity) (Ad-Dn-Nrdp1) largely inhibited I/R-induced cardiomyocyte apoptosis and inflammation (Fig. 2a, c).

Elevated cardiac Nrdp1 expression does not affect baseline cardiac function

Given our finding that Nrdp1 is upregulated with I/R injury, we sought to determine how the upregulated Nrdp-1 could contribute to cardiac injury in vivo. We generated transgenic mice expressing Flag-tagged Nrdp1 in the heart using the α-MHC promoter (Fig. 3a), We identified two independent transgenic founder lines, designated TG2 and TG6, in a C57BL/6 J background carrying human Nrdp1 gene (Fig. 3b). Western blot analysis with a monoclonal

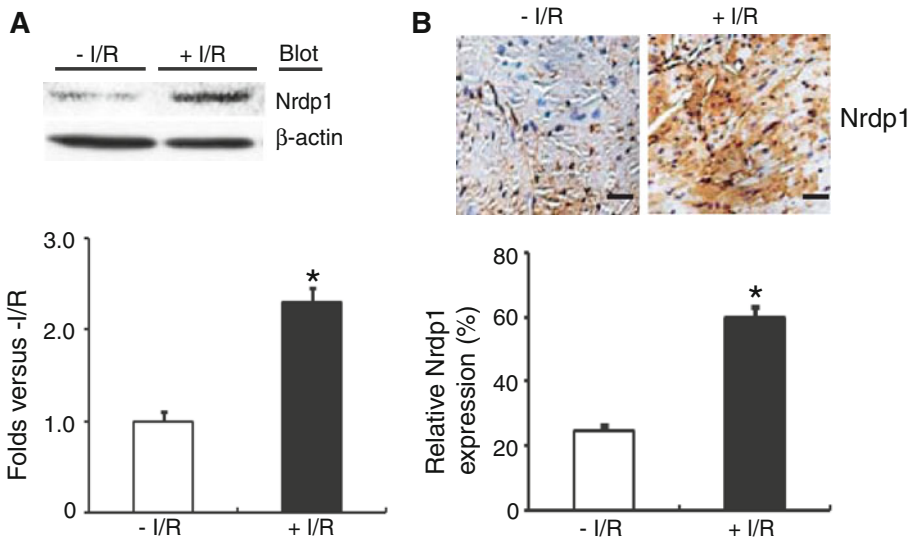

Fig. 1 Myocardial ischemic/reperfusion (I/R) injury increases Nrdp1 expression in the heart. **a** Western blot analysis of Nrdp1 and β-actin protein levels in hearts from control mice and I/R-treated mice with anti-Nrdp1 antibody (*top panel*). Quantitative analysis of protein bands shown in top panels (*bottom panel*, $n = 5$). *$P < 0.05$ versus control mice. **b** Heart sections from control mice and I/R-treated mice were stained with anti-Nrdp1 antibody (*top panel*). *Bar* 50 μm. Quantitative analysis of Nrdp1 expression of control mice and I/R-treated mice (*bottom panel*; $n = 3$). *$P < 0.05$ versus control mice

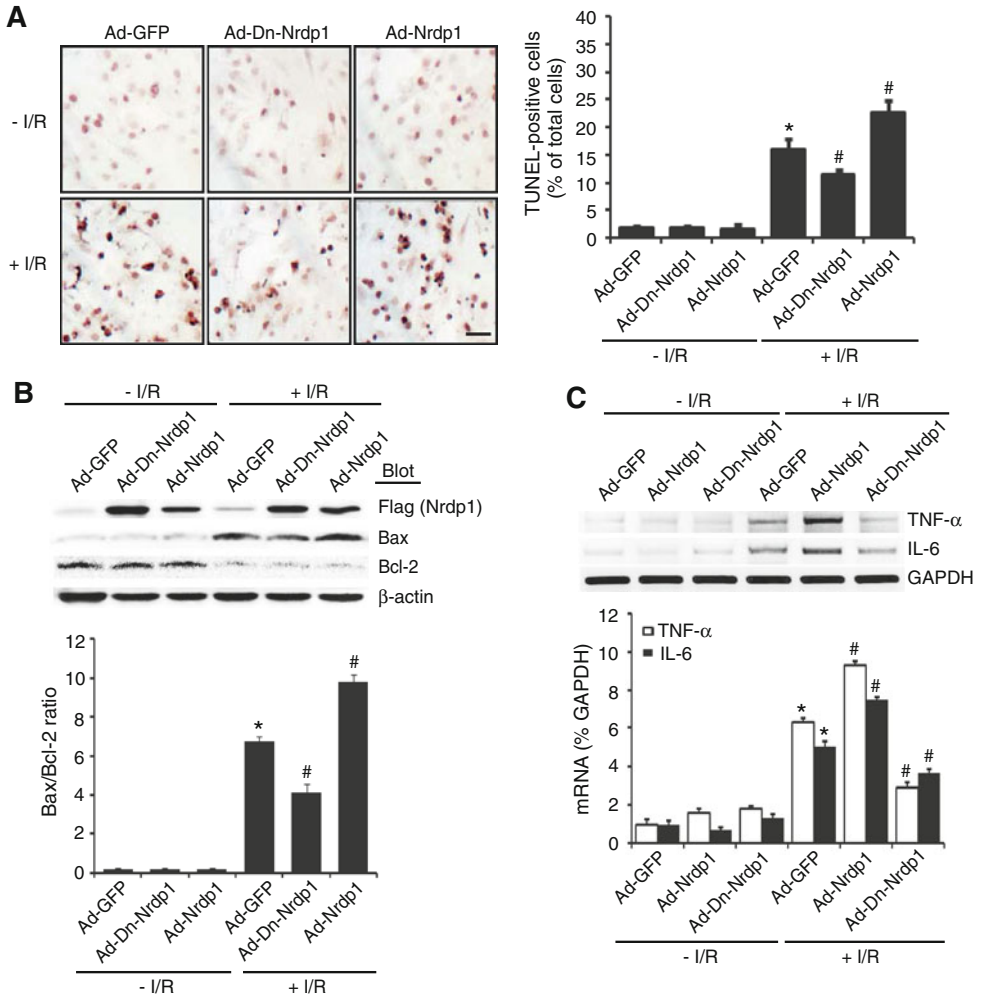

Fig. 2 Effect of Nrdp1 on apoptosis and expression of inflammatory cytokines after I/R in neonatal cardiomyocytes. **a** Cardiomyocytes were infected with Ad-GFP, Ad-Nrdp1 or Ad-Dn-Nrdp1 and exposed to 2-h ischemia followed by reperfusion for 24 h. Apoptotic cells were observed by TUNEL assay. A representative field is shown for each condition (*left panels*). Quantitative analysis of TUNEL-positive cells from three independent experiments (*right panel*); at least 120 cells per dish were counted. Results are expressed as mean ± SEM for three independent experiments. $^{*}P < 0.01$ versus. Ad-GFP. $^{\#}P < 0.01$ versus Ad-GFP + I/R. **b** Cardiomyocytes were infected as described and exposed to 2-h ischemia followed by reperfusion for 30 min. Western blot analysis of expression of Flag Nrdp1, Bax and Bcl-2 protein expression (*top panel*). Quantitative analysis of Bax/Bcl-2 ratio (*bottom panel*). **c** Cardiomyocytes were infected and treated as described. RT-PCR analysis of mRNA expression of TNF-α, IL-6 and GAPDH. Representative RT-PCR (*top panels*) and quantitative analysis (*bottom panel*). $^{*}P < 0.01$ versus Ad-GFP. $^{\#}P < 0.01$ versus Ad-GFP + I/R

antibody to the Flag epitope or anti-Nrdp1 antibody confirmed the Nrdp1 protein level in TG2 and TG6 higher by 1.4- and 2.8-fold, respectively, than that in WT hearts (Fig. 3c). Nrdp1 was expressed mostly in the heart, as compared with other organs, whereas Flag-Nrdp1 was expressed only in the heart and not in the lung, liver, spleen, kidney, or brain (Fig. 3d). Consistent with western blot results, immunohistochemical staining revealed the level of Nrdp1 significantly higher in cardiomyocytes of TG6 mice than in WT mice (Fig. 3e). The size and morphology of hearts from the two lines of transgenic mice appeared normal by H&E staining (data not shown). We observed no neonatal or adult death in transgenic mice. Cardiac function under the basal condition was similar for WT and TG6 mice (Supplementary Table 1). WT and TG2 mice did not differ in cardiac function, apoptosis or inflammation. Because Nrdp1 transgene expression in TG6 was similar to the level of endogenous Nrdp1 in the heart after I/R injury, TG6 mice were characterized extensively.

Cardiac Nrdp1 overexpression increases infarct size and mortality after I/R

To test whether overexpression of Nrdp1 enhances I/R-induced cardiac injury in vivo, we used TTC staining and determined infarct size by morphometric analysis 24 h

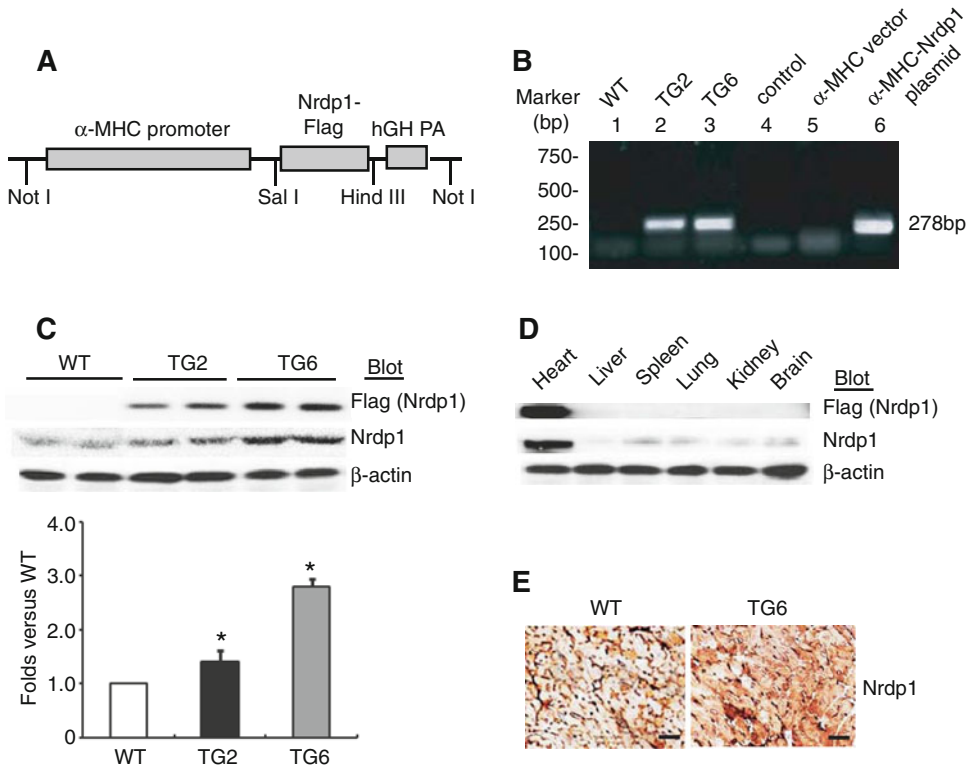

Fig. 3 Characterization of cardiac-specific Nrdp1 transgenic mice. **a** Schematic illustration of the cardiac α-myosin heavy chain promoter (MHC) promoter/Flag-Nrdp1 transgenic construct. Components of Nrdp1 transgene, including a 5.5-kb cardiac-specific mouse α-MHC promoter fragment, followed by a 1.0-kb human Nrdp1 cDNA with an N-terminal epitope tag (*Flag*) and a human growth-hormone polyadenylation (*PA*) sequence. **b** PCR analysis of wild-type mice (*WT, lane 1*) and mice with Nrdp1 TG2 (*lane 2*), TG6 (*lane 3*), control (*lane 4*), α-MHC promoter vector (*lane 5*) and α-MHC-Nrdp1 plasmid (*lane 6*). **c** Western blot analysis of exogenous Flag-Nrdp1 (*top panel*) and endogenous Nrdp1 (*bottom panel*) protein levels from hearts of WT, TG2, and TG6 mice. Quantitative analysis of protein bands shown in top panels (*bottom*, $n = 10$). *$P < 0.01$ versus WT mice. **d** Western blot analysis of Flag-Nrdp1 (*top panel*) and Nrdp1 (*bottom panel*) protein in extracts from heart, liver, spleen, lung, kidney, and brain tissues of a TG6 mouse. *β*-actin protein expression is shown as a loading control. **e** Ventricular sections from WT (*left panel*) and TG6 (*right panel*) mice stained with anti-Nrdp1 antibody. Brown staining indicates Nrdp1 expression. *Bar* 50 μm

after I/R. The infarct size, expressed as the ratio of infarct size to AAR and infarct size to LV, was significantly increased in TG6 mice as compared with WT mice (28.6 and 17.0% vs. 18.4 and 11.4%, $P < 0.05$) (Fig. 4a, b). In contrast, the proportion of LV area at risk (AAR/LV) was similar in WT mice and TG6 mice (62.0% and 61.3%) (Fig. 4b). Furthermore, survival after I/R was significantly lower for TG6 mice than for WT mice (68.4% [13/19] vs. 94.4% [17/18]) (Fig. 4c; $P < 0.05$), and the deaths in TG6 mice occurred during the early phases of reperfusion. We found no deaths in sham-operated groups (data not shown).

Cardiac Nrdp1 overexpression enhances myocardial apoptosis after I/R

Because apoptosis is a major event of I/R injury, we evaluated the effects of overexpressed Nrdp1 on apoptosis of injured hearts. Apoptotic cells were identified by TUNEL assay and DAPI staining, and staining with anti-α-sarcomeric actin was used to confirm myocyte identity. The percentage of TUNEL-positive cells in the I/R-injured myocardium at-risk area was higher in TG6 than in WT mice ($P < 0.05$) (Fig. 5a). In contrast, the number of TUNEL-positive cells in the hearts was similar in sham-operated groups. Furthermore, the levels of cleaved caspase-3 and cleaved PARP were higher in I/R-treated WT mice than in sham-operated WT mice. TG6 mice showed a significant increase in levels of cleaved caspase-3 and cleaved PARP as compared with WT mice after I/R (Fig. 5b).

To investigate further the effects of Nrdp1 on the regulation of pro- and anti-apoptotic protein expression, we examined the protein expression of Bcl-2 and Bax by western blot analysis. The baseline levels of Bax and Bcl-2 protein were similar in sham-operated WT and TG6 mice (Fig. 5c). After 24 h of I/R, Bcl-2 level was significantly decreased and Bax level was significantly increased in I/R-treated WT mice than in sham-operated WT mice. In

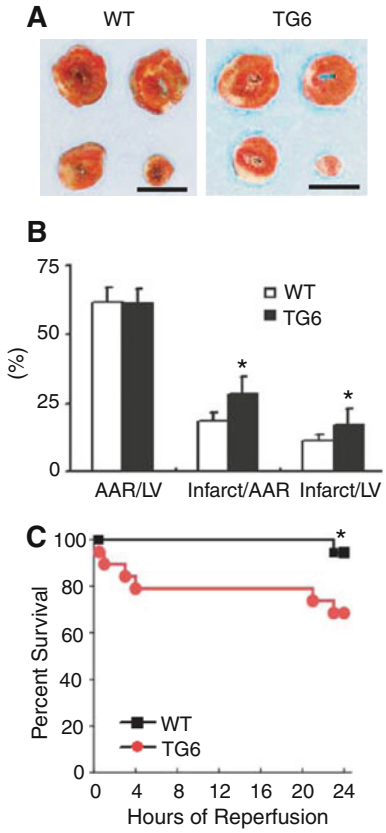

Fig. 4 Nrdp1 overexpression increases myocardial infarction size and mortality after I/R. **a** Representative photographs of TTC staining of myocardial sections from WT and TG6 mice after 30-min ischemia followed by 24-h reperfusion. The infarcted tissue stains pale white. *Bar* 5 mm. **b** Measurement of myocardial infarct size in WT and TG6 mice after I/R injury. Cumulative data indicating area at risk as a percentage of LV mass (AAR/LV) in WT and TG6 mice, area of infarction as a percentage of area at risk (infarct/AAR), and area of infarction as a percentage of left ventricular (LV) mass (infarct/LV) ($n = 6$). *$P < 0.05$ versus I/R-treated WT mice. **c** Survival in WT ($n = 18$) and TG6 mice ($n = 19$) undergoing 30 min of ischemia followed by 24 h of reperfusion as a function of time after onset of reperfusion. *$P < 0.05$, compared with TG6 mice

contrast, TG6 mice showed a marked downregulation of Bcl-2 and upregulation of Bax as compared with WT mice after I/R (Fig. 5c).

Cardiac Nrdp1 overexpression increases cardiac injury and inflammation

To assess the extent of cardiac injury and inflammation after I/R, sections from WT and TG6 mice were stained with H&E, and macrophage infiltration was characterized by immunohistochemical staining with Mac-2, a specific antibody for macrophages. Myocardial death and number of inflammatory cells did not differ between the sham-operated groups (Fig. 6a, b). However, 24 h after I/R, cardiomyocyte cytoarchitecture and cell degeneration were disrupted in TG6 mice as compared with WT mice (Fig. 6a, top and middle panels). Furthermore, TG6 mice showed a significant increase in number of neutrophils (Fig. 6a, bottom panel) and Mac-2-positive cells in the ischemic border of the myocardium as compared with WT mice (Fig. 6b).

Nrdp1 overexpression downregulates ErbB3 and its downstream targets

We first examined whether ErbB3 receptor was expressed in the mouse heart. ErbB3 mRNA was readily detectable in whole hearts by RT-PCR (Supplementary Fig. 1a). Furthermore, both western blot and immunohistochemical staining with ErbB3-specific antibody confirmed ErbB3 protein expressed in WT and TG6 mouse heart tissues (Supplementary Fig. 1b, c).

To elucidate the mechanism of cardiac-specific expression of Nrdp1 enhancing I/R injury, we determined the function of Nrdp1 by measuring the level of the Nrdp1 substrates ErbB3 receptor, BRUCE, MyD88, and TBK in injured hearts [7, 26, 27, 31]. The baseline levels of total and phosphorylated ErbB3 were similar between sham-operated WT and TG6 mice (Fig. 7a). After I/R, the levels of phosphorylated ErbB3 were significantly higher in WT mice than in sham-operated WT mice ($P < 0.01$, Fig. 7a). However, TG6 mice showed a markedly lower level of total and phosphorylated ErbB3 ($P < 0.01$). Interestingly, protein levels of cardiac BRUCE, MyD88 and TBK1 did not differ between sham-operated or I/R-treated animals (Supplementary Fig. 2).

ErbB3 regulates the activation of several protein kinases, including AKT, STAT3 and mitogen-activated protein kinases (MAPKs) involved in cell apoptosis [10]. We, therefore, measured the phosphorylation of these proteins with phospho-specific antibodies in heart extracts from WT and TG6 mice and found no significant difference in protein levels of phosphorylated AKT, ERK1/2, and STAT3 in WT and TG6 mice under the basal condition (Fig. 7b). I/R injury significantly increased the levels of phosphorylated AKT, ERK1/2, and STAT3 in WT mice. However, these effects were markedly suppressed in TG6 mice. To further confirm these observations in vitro, neonatal cardiomyocytes were infected with Ad-Nrdp1 or Ad-Dn-Nrdp1 and then underwent I/R. Levels of total ErbB3, total and phosphorylated AKT, STAT3, ERK1/2, p38 and JNK1/2 proteins did not differ between groups under the basal condition (Fig. 7c,d). After I/R treatment, Ad-Nrdp1 produced markedly decreased levels of total ErbB3, phosphorylated AKT, STAT3, and ERK1/2 and increased that of phosphorylated p38 and JNK1/2 as compared with the GFP control, whereas Ad-Dn-Nrdp1 had the opposite effect (Fig. 2a, c). These data indicate that Nrdp1 predominantly downregulates the ErbB3 pathway after I/R injury.

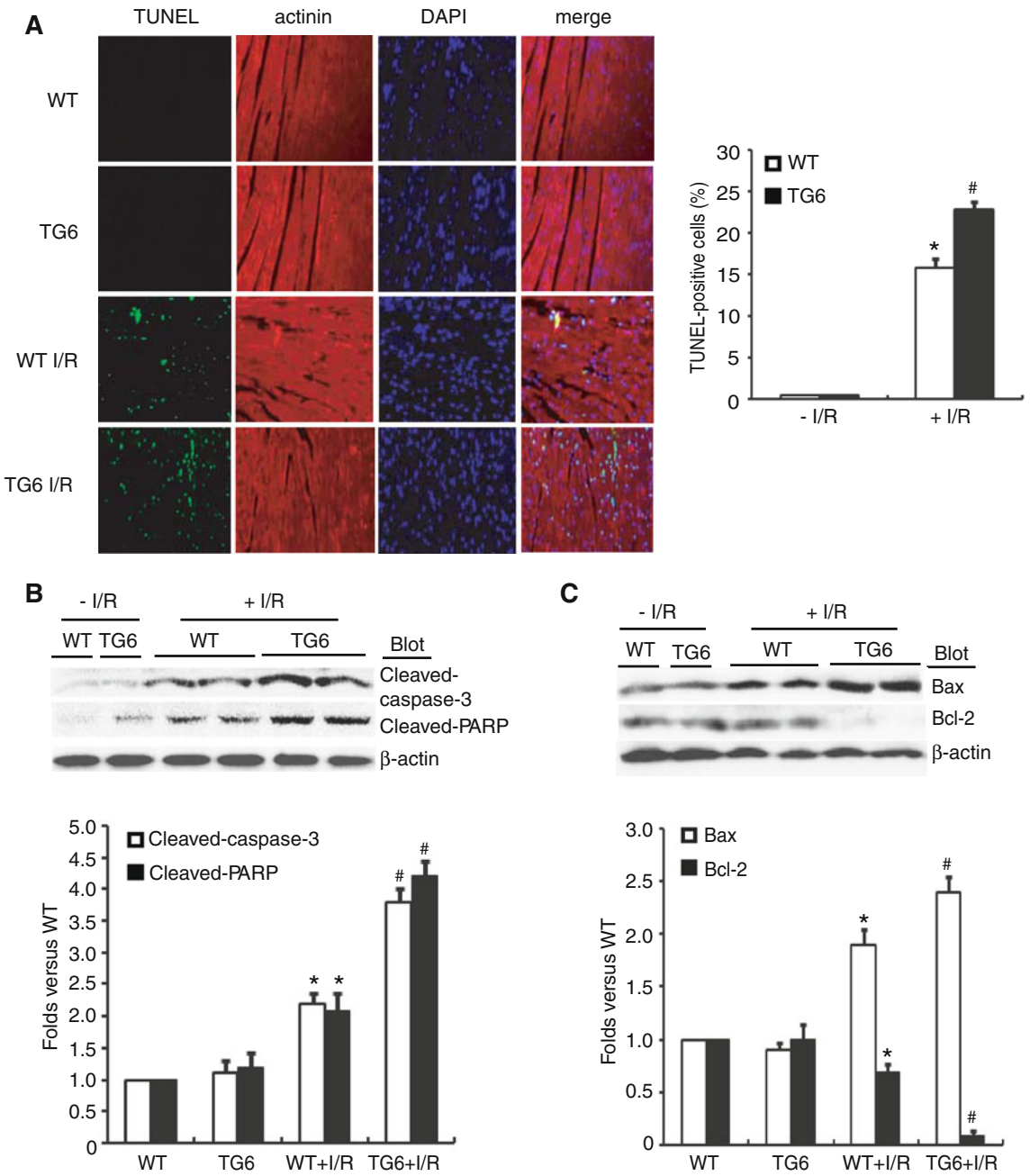

Fig. 5 Effect of Nrdp1 overexpression on cardiomyocyte apoptosis and expression of Bax and Bcl-2 after I/R injury. **a** Representative photomicrographs of cardiac cell apoptosis in myocardium in the ischemic border area examined by TUNEL assay (*green*). Myocytes were identified by immunostaining with anti-α-actin antibody (*red*), and nuclei were counterstained with DAPI (*blue*). For each sample, 6 fields (about 800 nuclei per field) were counted (×200). Histogram showing the quantitative analysis of TUNEL-positive cells from WT and TG6 mice. $^{*}P < 0.05$ versus I/R-treated WT mice ($n = 4$). **b** Representative western blots of cleaved caspase-3 and cleaved PARP proteins in the ischemic border myocardial area of WT and TG6 mice (*top panels*). Quantitative analysis of protein bands shown in top panels (*bottom panel*, $n = 5$). $^{*}P < 0.01$ versus WT mice; $^{\#}P < 0.01$ versus I/R-treated WT mice. **c** Representative western blots of Bax and Bcl-2 proteins from the ischemic myocardial border area of WT and TG6 mice (*top panels*). Quantitative analysis of protein bands shown in top panels (*bottom panel*, $n = 5$). $^{*}P < 0.01$ versus WT mice; $^{\#}P < 0.01$ versus I/R-treated WT mice

Discussion

In this report, we demonstrated that expression of endogenous Nrdp1, an E3 ligase, was significantly upregulated in the mouse heart after I/R. Overexpression of Nrdp1 significantly increased cardiomyocyte apoptosis and expression of inflammatory factors, whereas these effects were attenuated by a dominant-negative Nrdp1 mutant.

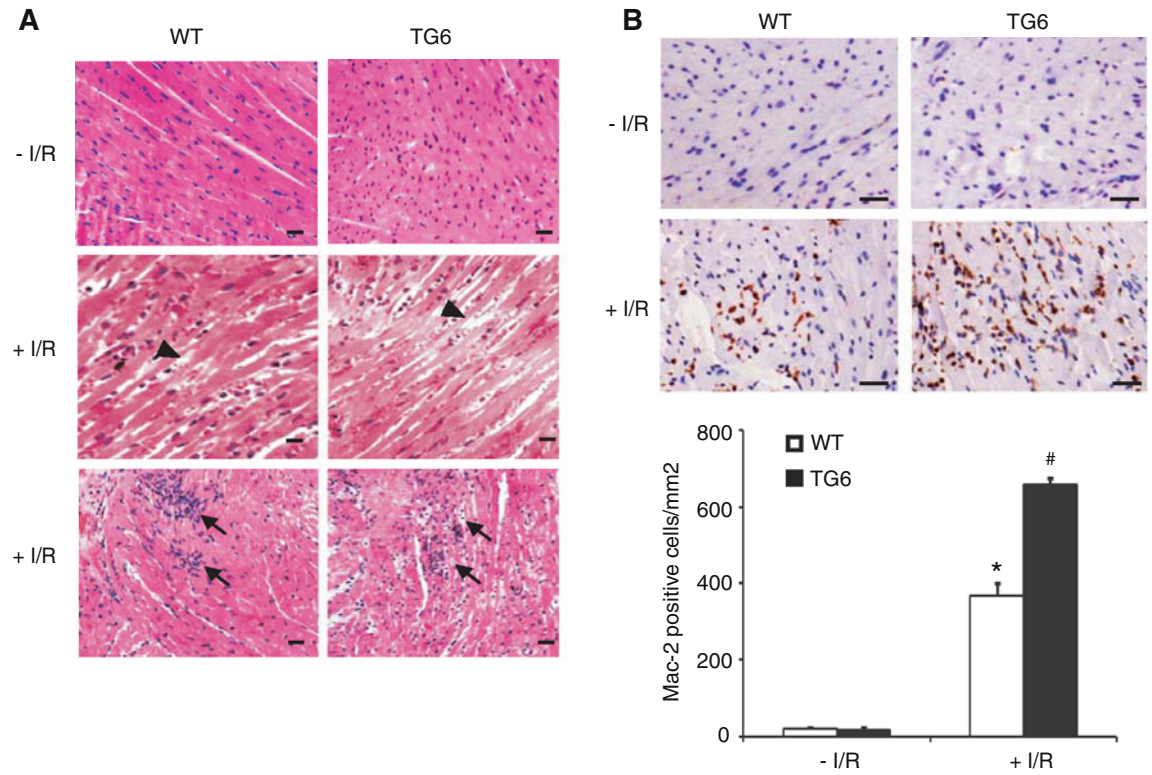

Fig. 6 Nrdp1 expression increases cardiomyocyte injury and inflammatory cell infiltration in mouse hearts after I/R injury. Representative histological analysis of WT left-ventricular (LV) sections ($n = 4$) and TG6 LV sections ($n = 4$) from WT and TG6 mice. **a** H&E-stained LV sections were from myocardium ischemic border area of WT and TG6 mice (*middle* and *bottom panels*). *Arrowheads* indicate the disruption of cardiomyocyte cytoarchitecture in the ischemic myocardial border area (*middle panels*). *Arrows* indicate neutrophil staining (*bottom panels*). *Bar* 50 μm. **b** Representative immunohistochemical staining with anti-Mac-2 antibody in the ischemic myocardial border area of WT and TG6 mice. Positive-stained cells were visualized with use of diaminobenzidine (*brown*). Mac-2-positive cells were quantified by digital image analysis. *Bar* 50 μm. Histogram of number of Mac-2-positive cells in the hearts of WT and TG6 mice (*bottom panels*). ($n = 5$). $^{*}P < 0.05$ versus WT mice; $^{\#}P < 0.01$ versus I/R-treated WT mice

Furthermore, cardiac-specific overexpression of Nrdp1 in vivo in mouse markedly increased infarct size, myocardial apoptosis, inflammatory cell infiltration, and mortality as compared with WT mice after I/R injury.

Previous studies suggested that the expression of Nrdp1 is inducible in cells in response to different stimuli and that its stability can be markedly enhanced by the de-ubiquitinating enzyme USP8 and ErbB3 ligand neuregulin 1 (NRG1) [6, 32]. In agreement with these observations, our results demonstrate that Nrdp1 protein level is upregulated in the mouse heart after I/R injury.

Apoptotic myocyte loss is a central feature of ischemic heart disease [8, 21, 22]. Nrdp1 promotes apoptosis in many cell types [27]; however, whether Nrdp1 enhances apoptosis in the heart after I/R injury was unknown. We found that increased expression of wild-type Nrdp1 promoted I/R-induced cardiomyocyte apoptosis, whereas adenoviral infection with the dominant-negative Nrdp1 in cardiomyocytes markedly inhibited this effect (Fig. 2a, b). Moreover, cardiac-specific expression of Nrdp1 led to a significant increase in myocardial infarct size, apoptosis and animal mortality after I/R injury (Figs. 4, 5a). In addition, the expression of cleaved caspase-3, cleaved PARP and Bax was significantly higher and that of Bcl-2 was lower in TG6 mice than in WT mice after I/R injury (Fig. 5b, c), which demonstrates that Nrdp1 promotes I/R-induced cardiomyocyte apoptosis.

The ErbB family of receptor tyrosine kinases (RTKs) contains four members—EGFR, ErbB2, ErbB3, and ErbB4—that play critical roles in cell cycle, proliferation and survival [10]. Transcripts of EGFR, ErbB2 and ErbB4 but not ErbB3 are expressed in neonatal and adult cardiac myocytes [10]. Interestingly, we found ErbB3 also expressed in the mouse heart. These findings are in agreement with the previous results from mouse heart tissues [14]. Gene targeting strategies in mice have highlighted the significance of the ErbB receptors in cardiac development and function [10]. Cardiac-specific ErbB2-knockout mice survived to adulthood but showed dilated cardiomyopathy at 3 months. Mice lacking ErbB4 die during mid-embryogenesis from the aborted development of myocardial trabeculae in the heart ventricle [10]. ErbB3-

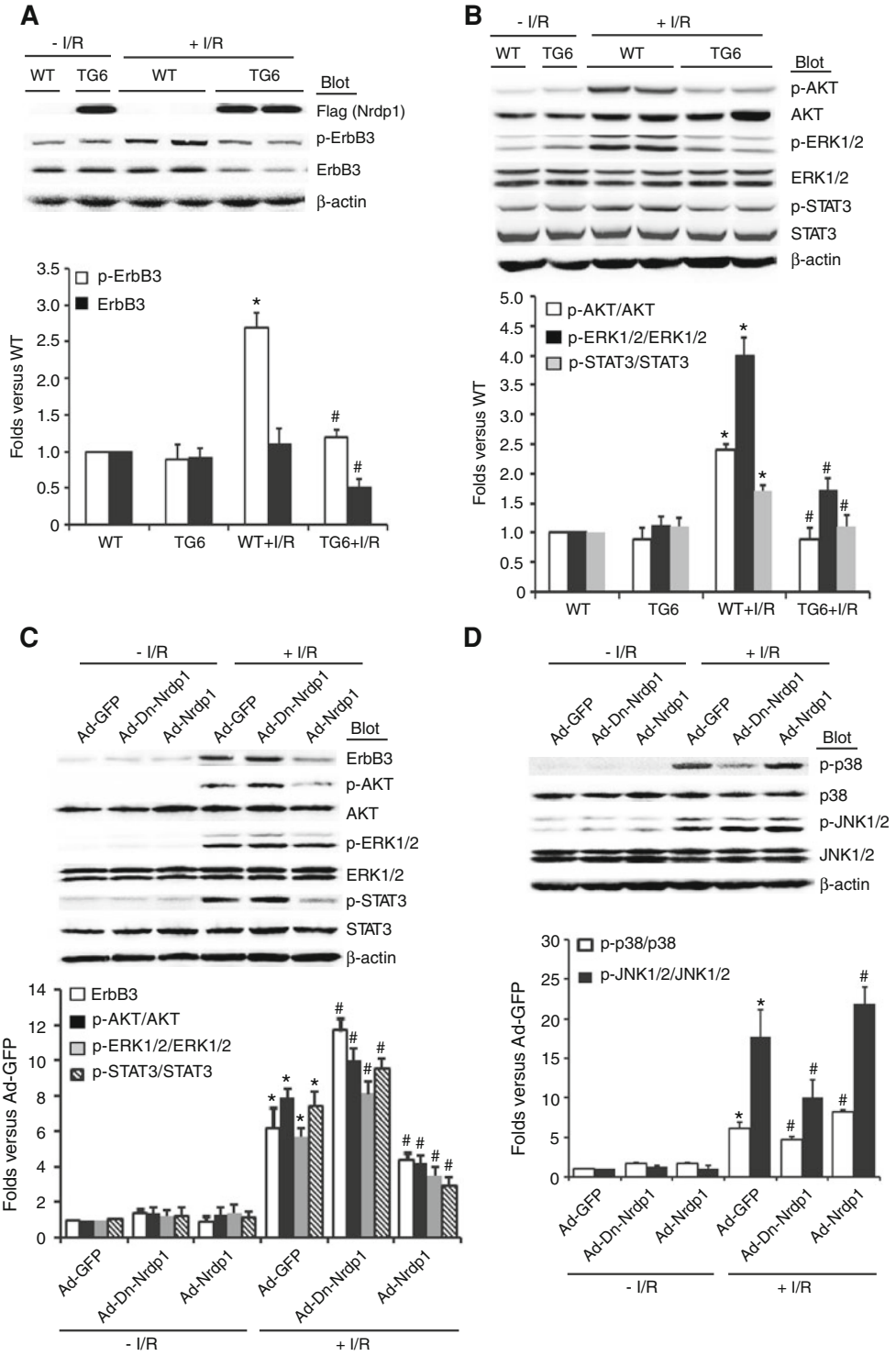

Fig. 7 Effect of Nrdp1 expression on ErbB3, AKT, STAT3, and MAPKs in vivo and in vitro after I/R. **a**, **b** Western blot analysis of protein levels of total and phosphorylated ErbB3, AKT, ERK1/2, and STAT3 from ischemic myocardial border area (*top panels*). Histograms show relative intensity of phosphorylated levels of ErbB3, AKT, ERK1/2, and STAT3 (*bottom panels*) ($n = 5$). $^{*}P < 0.01$ versus WT mice; $^{\#}P < 0.01$ versus I/R-treated WT mice. **c** Cardiomyocytes were infected with Ad-GFP or Ad-Nrdp1 or Ad-Dn-Nrdp1 and exposed to 2-h ischemia followed by 30-min reperfusion. Western blot analysis of protein levels as in **a**, **b** (*top panels*). Histograms show relative intensity of phosphorylated proteins (*bottom panels*) ($n = 3$). **d** Cardiomyocytes were infected and treated as in c. Representative western blots show levels of total and phosphorylated p38 and JNK1/2 (*top panels*). Histograms show relative intensity of phosphorylated proteins (*bottom panels*) ($n = 3$). $^{*}P < 0.01$ versus Ad-GFP; $^{\#}P < 0.01$ versus Ad-GFP + I/R

null mice exhibit hypoplastic endocardial cushions leading to death at mid-gestation [28]. Emerging biochemical data demonstrate that ErbB receptor dimerization results in auto- and trans-phosphorylation of intracellular domains. The phosphorylated forms of these receptors then can serve as docking sites for distinct cytoplasmic proteins involved in transducing downstream signaling cascades. Unlike other ErbB receptors, ErbB3 lacks intrinsic kinase activity. Upon ligand binding, ErbB3 can be transactivated on cytoplasmic tyrosine residues by dimerization with other ErbB family members [23]. Recent studies demonstrate that Nrdp1 associates specifically with ErbB3 and regulates a steady-state level of this receptor via proteasomes, thereby influencing neuregulin signaling-dependent cell

survival [6, 7, 34]. Our results of cultured cardiomyocytes and TG6 mice demonstrate that increased expression of Nrdp1 markedly downregulated levels of ErbB3 protein after I/R injury, but dominant-negative Nrdp1 attenuated this effect (Fig. 7a, c). Thus, Nrdp1 plays an important role in regulation of ErbB3 protein levels in the heart during I/R injury.

Various cardioprotective mechanisms have been proposed during I/R, including activation of the G-protein-coupled receptors (GPCR)/PI3 K/AKT/eNOS pathway, gp130/janus kinase (JAK)/signal transducer and activator of transcription 3 (STAT3) pathway, and reperfusion injury salvage kinase (RISK) pathway [13, 14, 29]. However, the specific RISK kinases that confer the protective effect by postconditioning are controversial in different species [13, 14, 29]. For example, RISK activation is not important for postconditioning in pigs [29]. The PI3 K/AKT pathway is a target of I/R injury and plays a critical role in cell survival by inhibiting caspase-mediated apoptosis [1, 2]. MAPKs include extracellular signal-regulated kinase 1/2 (ERK1/2), c-Jun N-terminal protein kinase 1/2 (JNK1/2), and p38 MAPK, which are the major mediators of intracellular signals in response to various stimuli, such as I/R injury [1, 2]. Specifically, inhibition of JNK and p38 MAPK has been implicated in stress-responsive signaling preventing the initiation of cardiac injury [1, 2]. In contrast, sustained activation of ERK is necessary for cardiomyocyte survival [1, 2]. STAT proteins are part of the gp130/JAK/STAT pathway, which mediates the transduction of stress signals from the plasma membrane to the nucleus. In the heart, the JAK-STAT pathway is involved in I/R injury, hypertrophy, and post-partum cardiomyopathy. STAT3 is central for the initial stages of cardiomyogenesis, and STAT3 knockout causes embryonic lethality. Cardiac-specific overexpression of constitutively active STAT3 reduces infarct size, whereas STAT3-knockout mice show larger infarcts, which supports the cardioprotective role of STAT3 [3]. Importantly, several pathways activated by ErbB ligands are the RAS/MEK/ERK and PI3 K/AKT pathways and STAT3, and these pathways are responsible for cardiac cell survival [10]. Our TG6 mice showed pronounced inhibition of activation of AKT, ERK1/2 and STAT3 after I/R injury (Fig. 7a, b). The data from in vitro cardiomyocytes further demonstrated that increased expression of Nrdp1 inhibited I/R-triggered activation of AKT, ERK1/2 and STAT3 but enhanced p38 MAPK and JNK1/2 phosphorylation. In contrast, dominant-negative Nrdp1 attenuated these effects (Fig. 7c, d). Thus, Nrdp1 plays a critical role in regulation of ErbB3 and its downstream signaling pathways in the heart during I/R.

In addition to ErbB3, Nrdp1 might promote ubiquitination and degradation of other protein(s) such as BRUCE/Apollon, a large membrane-associated inhibitor-of-apoptosis domain-containing protein that may be involved in the regulation of apoptosis [12, 27]. We found no significant difference between WT and TG6 mice in protein levels of BRUCE under the basal condition or after I/R (Supplementary Fig. 2), which suggests that BRUCE may not be involved in Nrdp1-mediated cardiomyocyte apoptosis after I/R. Thus, Nrdp1 seems to have a pro-apoptotic effect on I/R-induced cardiac injury predominantly by promoting degradation of the ErbB3 receptor and its downstream targets.

Inflammation is an important cause of I/R-induced cardiac injury, and the innate immune response to I/R is the most common cause of myocardial inflammation. The TLR4/MyD88-dependent signaling pathway plays a critical role in modulating cardiac inflammation and injury [9, 11, 19]. The importance of inflammatory cell recruitment in the pathophysiologic features of myocardial reperfusion injury was demonstrated in animal models [4]. Recent study has demonstrated that Nrdp1 plays a critical role in modulating the TLR-mediated inflammation response [31]. However, the effect of Nrdp1 in myocardial I/R injury is incompletely defined. We demonstrated that overexpression of Nrdp1 promoted I/R-induced expression of inflammatory cytokines, but this effect was inhibited by dominant-negative Nrdp1 adenoviral infection (Fig. 2c). Furthermore, Nrdp1 transgenic mouse hearts showed significantly increased accumulation of neutrophils and macrophages after I/R injury (Fig. 6). However, Nrdp1 expression had no impact on myocardial MyD88 and TBK1 protein levels (Supplementary Fig. 2), which suggests that Nrdp1-mediated myocardial inflammation after I/R injury may not depend on MyD88 and TBK1. Our results also suggest that Nrdp1-mediated downregulation of its substrate proteins may depend on different tissue types and pathological conditions. Indeed, Wang et al. [31] recently reported that Nrdp1 directly bound and polyubiquitinated MyD88 and TBK1, which led to degradation of MyD88 and activation of TBK1, but Nrdp1 did not affect TBK1 protein levels.

In conclusion, our findings demonstrate an important role of Nrdp1 in the pathogenesis of I/R-induced myocardial injury. Overexpression of Nrdp1 in the heart increased infarction size, myocardial apoptosis, and inflammation after I/R injury. These effects might be a result of a rapid inactivation of cardiac ErbB3 and alteration of the levels of downstream targets. Thus, targeted therapy to decrease Nrdp1 expression in the heart may help ameliorate ischemic myocardial injury.

Acknowledgments This work was supported by grants from China National Natural Science Funds for Distinguished Young Scholars (81025001; HL, 30888004; JD) and the Beijing high-level talents program (PHR20110507; HL).

Conflict of interest None.

References

1. Armstrong SC (2004) Protein kinase activation and myocardial ischemia/reperfusion injury. Cardiovasc Res 61:427–436. doi: 10.1016/j.cardiores.2003.09.031S000863630300662x
2. Baines CP, Molkentin JD (2005) STRESS signaling pathways that modulate cardiac myocyte apoptosis. J Mol Cell Cardiol 38:47–62 (S0022-2828(04)00325-6)
3. Boengler K, Hilfiker-Kleiner D, Drexler H, Heusch G, Schulz R (2008) The myocardial JAK/STAT pathway: from protection to failure. Pharmacol Ther 120:172–185 (S0163-7258(08)00140-x)
4. Bowden RA, Ding ZM, Donnachie EM, Petersen TK, Michael LH, Ballantyne CM, Burns AR (2002) Role of alpha4 integrin and VCAM-1 in CD18-independent neutrophil migration across mouse cardiac endothelium. Circ Res 90:562–569. doi:10.1161/01.RES.0000013835.53611.97
5. Camenisch TD, Schroeder JA, Bradley J, Klewer SE, McDonald JA (2002) Heart-valve mesenchyme formation is dependent on hyaluronan-augmented activation of ErbB2-ErbB3 receptors. Nat Med 8:850–855. doi:10.1038/nm742nm742
6. Cao Z, Wu X, Yen L, Sweeney C, Carraway KL 3rd (2007) Neuregulin-induced ErbB3 downregulation is mediated by a protein stability cascade involving the E3 ubiquitin ligase Nrdp1. Mol Cell Biol 27:2180–2188 (MCB.01245-06)
7. Diamonti AJ, Guy PM, Ivanof C, Wong K, Sweeney C, Carraway KL 3rd (2002) An RBCC protein implicated in maintenance of steady-state neuregulin receptor levels. Proc Natl Acad Sci USA 99:2866–2871. doi:10.1073/pnas.052709799
8. Eefting F, Rensing B, Wigman J, Pannekoek WJ, Liu WM, Cramer MJ, Lips DJ, Doevendans PA (2004) Role of apoptosis in reperfusion injury. Cardiovasc Res 61:414–426. doi:10.1016/j.cardiores.2003.12.023S0008636303007910
9. Feng Y, Zhao H, Xu X, Buys ES, Raher MJ, Bopassa JC, Thibault H, Scherrer-Crosbie M, Schmidt U, Chao W (2008) Innate immune adaptor MyD88 mediates neutrophil recruitment and myocardial injury after ischemia-reperfusion in mice. Am J Physiol Heart Circ Physiol 295:H1311–H1318 (00119.2008)
10. Fuller SJ, Sivarajah K, Sugden PH (2008) ErbB receptors, their ligands, and the consequences of their activation and inhibition in the myocardium. J Mol Cell Cardiol 44:831–854 (S0022-2828(08)00343-x)
11. Ha T, Hua F, Li Y, Ma J, Gao X, Kelley J, Zhao A, Haddad GE, Williams DL, Browder IW, Kao RL, Li C (2006) Blockade of MyD88 attenuates cardiac hypertrophy and decreases cardiac myocyte apoptosis in pressure overload-induced cardiac hypertrophy in vivo. Am J Physiol 290:H985–994 (00720.2005)
12. Hauser HP, Bardroff M, Pyrowolakis G, Jentsch S (1998) A giant ubiquitin-conjugating enzyme related to IAP apoptosis inhibitors. J Cell Biol 141:1415–1422. doi:10.1083/jcb.141.6.1415
13. Heusch G (2009) No risk, no… cardioprotection? A critical perspective. Cardiovasc Res 84:173–175 (cvp298)
14. Heusch G, Boengler K, Schulz R (2008) Cardioprotection: nitric oxide, protein kinases, and mitochondria. Circulation 118:1915–1919. doi:118/19/1915
15. Hosoda T, Kajstura J, Leri A, Anversa P (2010) Mechanisms of myocardial regeneration. Circ J 74:13–17. doi:JST.JSTAGE/circj/CJ-09-0665
16. Li F, Xie P, Fan Y, Zhang H, Zheng L, Gu D, Patterson C, Li H (2009) C terminus of Hsc70-interacting protein promotes smooth muscle cell proliferation and survival through ubiquitin-mediated degradation of FoxO1. J Biol Chem 284:20090–20098. doi: M109.017046
17. Li HH, Kedar V, Zhang C, McDonough H, Arya R, Wang DZ, Patterson C (2004) Atrogin-1/muscle atrophy F-box inhibits calcineurin-dependent cardiac hypertrophy by participating in an SCF ubiquitin ligase complex. J Clin Invest 114:1058–1071. doi: 10.1172/JCI22220
18. Li HH, Willis MS, Lockyer P, Miller N, McDonough H, Glass DJ, Patterson C (2007) Atrogin-1 inhibits Akt-dependent cardiac hypertrophy in mice via ubiquitin-dependent coactivation of Forkhead proteins. J Clin Invest 117:3211–3223. doi:10.1172/JCI31757
19. Li T, Wang Y, Liu C, Hu Y, Wu M, Li J, Guo L, Chen L, Chen Q, Ha T, Li C, Li Y (2009) MyD88-dependent nuclear factor-kappaB activation is involved in fibrinogen-induced hypertrophic response of cardiomyocytes. J Hypertens 27:1084–1093. doi: 10.1097/HJH.0b013e3283293c93
20. Liao YH, Cheng X (2006) Autoimmunity in myocardial infarction. Int J Cardiol 112:21–26 (S0167-5273(06)00560-2)
21. Logue SE, Gustafsson AB, Samali A, Gottlieb RA (2005) Ischemia/reperfusion injury at the intersection with cell death. J Mol Cell Cardiol 38:21–33 (S0022-2828(04)00330-x)
22. Lopez-Neblina F, Toledo AH, Toledo-Pereyra LH (2005) Molecular biology of apoptosis in ischemia and reperfusion. J Invest Surg 18:335–350 (K3574075H438W921)
23. Negro A, Brar BK, Lee KF (2004) Essential roles of Her2/erbB2 in cardiac development and function. Recent Prog Horm Res 59:1–12. doi:10.1210/rp.59.1.1
24. Opie LH, Commerford PJ, Gersh BJ, Pfeffer MA (2006) Controversies in ventricular remodelling. Lancet 367:356–367 (S0140-6736(06)68074-4)
25. Orlowski RZ (1999) The role of the ubiquitin-proteasome pathway in apoptosis. Cell Death Differ 6:303–313. doi:10.1038/sj.cdd.4400505
26. Qiu XB, Goldberg AL (2002) Nrdp1/FLRF is a ubiquitin ligase promoting ubiquitination and degradation of the epidermal growth factor receptor family member, ErbB3. Proc Natl Acad Sci USA 99:14843–14848. doi:10.1073/pnas.232580999
27. Qiu XB, Markant SL, Yuan J, Goldberg AL (2004) Nrdp1-mediated degradation of the gigantic IAP, BRUCE, is a novel pathway for triggering apoptosis. EMBO J 23:800–810. doi: 10.1038/sj.emboj.7600075
28. Riethmacher D, Sonnenberg-Riethmacher E, Brinkmann V, Yamaai T, Lewin GR, Birchmeier C (1997) Severe neuropathies in mice with targeted mutations in the ErbB3 receptor. Nature 389:725–730. doi:10.1038/39593
29. Skyschally A, van Caster P, Boengler K, Gres P, Musiolik J, Schilawa D, Schulz R, Heusch G (2009) Ischemic postconditioning in pigs: no causal role for RISK activation. Circ Res 104:15–18 (CIRCRESAHA.108.186429)
30. Toth A, Nickson P, Qin LL, Erhardt P (2006) Differential regulation of cardiomyocyte survival and hypertrophy by MDM2, an E3 ubiquitin ligase. J Biol Chem 281:3679–3689 (M509630200)
31. Wang C, Chen T, Zhang J, Yang M, Li N, Xu X, Cao X (2009) The E3 ubiquitin ligase Nrdp1 'preferentially' promotes TLR-mediated production of type I interferon. Nat Immunol 10:744–752 (ni.1742)
32. Wu X, Yen L, Irwin L, Sweeney C, Carraway KL 3rd (2004) Stabilization of the E3 ubiquitin ligase Nrdp1 by the deubiquitinating enzyme USP8. Mol Cell Biol 24:7748–7757. doi: 10.1128/MCB.24.17.7748-7757.200424/17/7748
33. Xie P, Guo S, Fan Y, Zhang H, Gu D, Li H (2009) Atrogin-1/MAFbx enhances simulated ischemia/reperfusion-induced apoptosis in cardiomyocytes through degradation of MAPK phosphatase-1 and sustained JNK activation. J Biol Chem 284:5488–5496 (M806487200)

34. Yen L, Cao Z, Wu X, Ingalla ER, Baron C, Young LJ, Gregg JP, Cardiff RD, Borowsky AD, Sweeney C, Carraway KL 3rd (2006) Loss of Nrdp1 enhances ErbB2/ErbB3-dependent breast tumor cell growth. Cancer Res 66:11279–11286 (66/23/11279)
35. Yet SF, Tian R, Layne MD, Wang ZY, Maemura K, Solovyeva M, Ith B, Melo LG, Zhang L, Ingwall JS, Dzau VJ, Lee ME, Perrella MA (2001) Cardiac-specific expression of heme oxygenase-1 protects against ischemia and reperfusion injury in transgenic mice. Circ Res 89:168–173. doi:10.1161/hh1401.093314
36. Zhang C, Xu Z, He XR, Michael LH, Patterson C (2005) CHIP, a cochaperone/ubiquitin ligase that regulates protein quality control, is required for maximal cardioprotection after myocardial infarction in mice. Am J Physiol Heart Circ Physiol 288:H2836–H2842 (01122.2004)